Int. J. Solids Structures Vol. 22, No. 5, pp. 511–526, 1986
Printed in Great Britain.

0020-7683/86 $3.00+.00
Pergamon Journals Ltd.

WAVELENGTH SELECTION IN THE POSTBUCKLING OF A LONG RECTANGULAR PLATE

N. DAMIL and M. POTIER-FERRY
Université Hassan II, Faculté des Sciences II, Ben M'Sik, Casablanca, Maroc and
Laboratoire de Physique et Mécanique des Matériaux, Faculté des Sciences de Metz, Ile du Saulcy, 57045 Metz Cedex 1, France

(*Received* 25 *October* 1984)

Abstract—We study the postbuckling of an elastic rectangular plate with a large aspect ratio. Using the multiple scale expansion method, we establish that, for each postcritical load, the wavelength of buckling patterns is restricted to some band. The results are compared with experiments and with those given by the classical postbuckling theory.

1. INTRODUCTION

We study the buckling of an elastic rectangular plate with a large aspect ratio subjected to uniaxial compression. The long sides, parallel to the $0x$-axis, are simply supported. Various boundary conditions are considered along the short sides. In classical linear theory[1, 2], the latter boundary conditions are not taken into account and the assumed mode is periodic with respect to x. For a given wavenumber q, the plane state is unstable when the load λ exceeds a critical value $\lambda(q)$. The classical postbuckling theory[3, 4] can be applied if the aspect ratio is finite, or if one, *a priori*, seeks periodic postbuckling solutions with a prescribed wavenumber. In the case of a single buckling mode, this nonlinear theory provides a solution whose shape is roughly constant and whose amplitude grows as $\varepsilon^{1/2}$, ε being the difference between the load and its critical value. Similar methods have been applied for aspect ratios close to $2^{1/2}, 6^{1/2}, \ldots$, in which cases two modes with two different wavelengths are competing[5–10]. According to the boundary conditions, the stable solutions correspond either to any of the wavelengths or to both. The coexistence of different types of solutions has been also established away from the first bifurcation point by numerical computations[8, 11, 12].

In the present case of a large aspect ratio, many buckling modes are competing, and those methods do not work. The multiple scale expansion method will permit us to take this mode packet into account and to select a band of admissible wavelengths.

Experiments have been performed with clamped short sides by Clement *et al.*[13] and with simply supported short sides by Boucif *et al.*[14]. The observed values of (λ, q) are not in the whole region above the neutral stability curve $\lambda(q)$. With clamped short sides, the selected wavenumbers seem to be inside a cone that is pictured in Fig. 1. Furthermore, the postbuckling deflection is not exactly periodic, but its amplitude is modulated close to the short sides. In the simply supported case, this deflection is periodic, and the observed values of (λ, q) are in the region above a parabolic-looking curve, which is narrower than the neutral stability curve (Fig. 1).

The amplitude modulation is now well understood and can be elucidated by solving an amplitude equation that has been established by Segel[15], Newell and Whitehead[16] for Rayleigh–Bénard's convection and by Lange and Newell[17] for a beam buckling problem. This amplitude equation method has been recently extended by Cross *et al.*[18] and by Pomeau and Zaleski[19]. In this way, they have explained the existence of a large number of solutions beyond the instability threshold, the selected values of (λ, q) lying in a cone as pictured in Fig. 1. The limits of this cone are very sensitive to the boundary conditions on the long sides, as also on the short sides, which seems more surprising. This analysis has been applied to the convection[18] and to various buckling problems of a beam on a foundation[19–22].

The wavelength selection problem in the buckling of a long rectangular plate has been previously considered by Pomeau[23] with clamped short sides and with in-plane

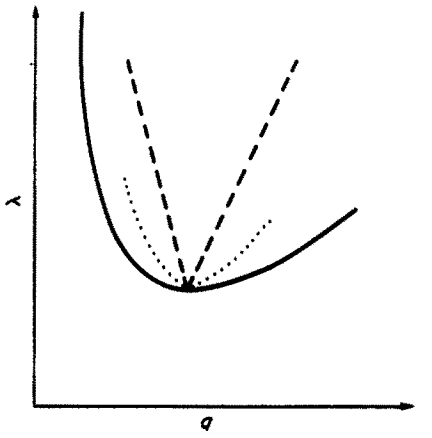

Fig. 1. Stability boundaries in the wavenumber–load plane. The continuous line is the classical neutral stability curve. The two others are lower limits with clamped (dashes, reference [13]) and simply supported (dots, reference [14]) short sides.

boundary conditions different from those of the experiments. In the present paper, we solve this wavelength selection with more realistic boundary conditions. Furthermore, we discuss the influence of the short side boundary conditions. We use a double scale expansion method, as introduced by Cross *et al.*[18] and as modified in [22].

2. THE PHYSICAL PROBLEM AND LINEAR STABILITY

We consider a thin elastic rectangular plate of length L and of width π, in nondimensional terms. The length L is assumed to be large. A uniform compressive load is applied on the short sides so that the prebuckling stress is uniaxial and uniform (Fig. 2). Within the framework of Von Karman plate theory, the transverse displacement w and the additional stress function f are solutions of

$$\Delta^2 w + \lambda \partial_x^2 w - [w, f] = 0, \tag{1}$$

$$\Delta^2 f = -[w, w]/2, \tag{2}$$

where $[\,,\,]$ is the usual bracket operator,

$$[g, h] = (\partial_x^2 g)(\partial_y^2 h) + (\partial_y^2 g)(\partial_x^2 h) - 2(\partial_{xy}^2 g)(\partial_{xy}^2 h), \tag{3}$$

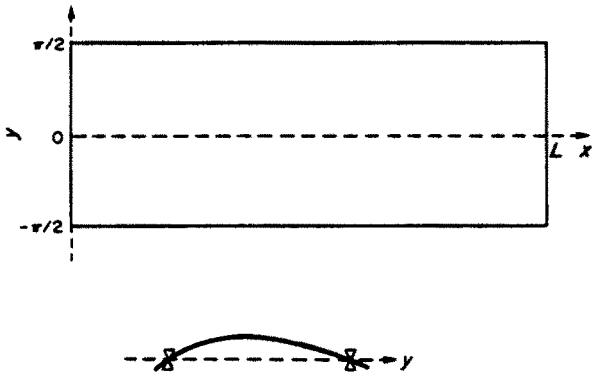

Fig. 2. Plate geometry and long sides boundary conditions.

$\lambda = 12Nla^2(1-\nu^2)/Eh^3\pi^2$ is the load parameter,
N is the applied compressive force per unit length,
la, h are the width and thickness of the plate,
E, ν are Young's modulus and Poisson's ratio of the plate material.

In the experiments reported in [13] and [14], the transverse displacement along the long sides is restrained by rigid vertical blades (Fig. 2). This implies that this part of the boundary is simply supported

$$w(x, \pm\pi/2) = \partial_y^2 w(x, \pm\pi/2) = 0, \tag{4}$$

and that no in-plane stress is applied there

$$f(x, \pm\pi/2) = \partial_y f(x, \pm\pi/2) = 0. \tag{5}$$

Boundary conditions similar to (5) must be satisfied along the short sides, but they are not needed in our calculations. Pomeau[23] postulated that there is no in-plane shear stress and that the normal displacement is uniform on each side, which leads to the alternative boundary conditions[10]

$$\partial_y f(x, \pm\pi/2) = \partial_y^3 f(x, \pm\pi/2) = 0. \tag{6}$$

The short sides are assumed to be perfectly or imperfectly clamped

$$w(0,y) = w(L,y) = 0, \tag{7}$$

$$(\partial_x w - k\partial_x^2 w)(0,y) = 0, \qquad (\partial_x w + k\partial_x^2 w)(L,y) = 0. \tag{8}$$

The nonnegative coefficient k measures the flexural compliance of the support. The simply supported case $k = \infty$ will be studied in Section 5.

Within the standard linear theory[1, 2], the critical value of the load λ is characterized by the existence of a buckling mode $W(x,y)$, which is a solution of the linearized equation

$$\Delta^2 W + \lambda \partial_x^2 W = 0 \tag{9}$$

and, in theory, of boundary conditions (4), (7) and (8). Because the aspect ratio is large, the conditions on the short sides act as perturbations and therefore can be neglected in a first-order analysis. Conditions (7) and (8) are replaced by the requirement of a harmonic behaviour in the x-direction. With this method, the first packet of buckling modes can be expressed as

$$W(x,y) = e^{iqx} \cos y + \text{c.c.}, \tag{10}$$

$$\lambda(q) = (q + 1/q)^2, \tag{11}$$

where c.c. denotes the complex conjugate. One finds other packets by replacing $\cos y$ by $\sin(2y)$, $\cos(3y), \ldots$, but the corresponding values of $\lambda(q)$ are much greater than the one given by (10), (11). The neutral stability curve has the same shape as in Fig. 1. The critical load and the critical wavenumber correspond to the minimum of this curve

$$\lambda_c = 4, \qquad q_c = 1.$$

The validity of this first-order analysis arises from the large aspect ratio and from the uniformity of the prebuckling state. Indeed, the latter property allows a Fourier splitting that justifies the requirement of the harmonic mode. It is a straightforward matter that, when the load is greater than λ_c, an initial displacement in the form (11) is dynamically

amplified for a band of wavenumbers close to q_c. Then we have to solve a bifurcation problem with a continuous spectrum.

3. TWO AMPLITUDE EQUATIONS

In this section we perform an asymptotic analysis, the main small parameter being the load increment

$$\varepsilon = \lambda - \lambda_c = \lambda - 4. \tag{12}$$

When ε is positive, there is a large number of instability modes. The bandwidth of the corresponding wavenumbers is $O(\varepsilon^{1/2})$, as indicated by Fig. 1. A linear combination of these modes leads to a slowly modulated spatial oscillation. That is why one usually seeks solutions which depend on x, y and, furthermore, on X defined by[16, 17, 24]

$$X = \varepsilon^{1/2} x. \tag{13}$$

This slow variable will permit us to take into account the boundary conditions on the short sides that had been neglected in the first-order analysis.

Unfortunately, Cross *et al.*[18] established that such an asymptotic expansion does not converge for large X. In this region of a large X, they first used an alternative double scale expansion, and next they matched the two types of solutions. A more general method would be to introduce a larger number of scales x, $\varepsilon^{1/2}x$, $\varepsilon x, \ldots$, but the computations would become more intricate than those in [18].

In view of experimental results[13] and previous computations[18, 20], we expect that the deflection goes to a periodic shape in the centre of the plate. The corresponding wavenumber must not be *a priori* prescribed since the problem is nonlinear. Hence, as in [22], we introduce a new variable ξ that is able to account exactly for a periodic behaviour in the centre

$$\xi = q(\varepsilon)x, \qquad q(\varepsilon) = 1 + Q_1\varepsilon + Q_2\varepsilon^{3/2} + \cdots. \tag{14}$$

The real numbers $Q_1, Q_2, \ldots$ are to be specified later on. We seek the deflection w and the stress function f as depending on X, ξ, y, and we shall require 2π-periodicity with respect to ξ. This choice will provide uniformly valid solutions in the semi-infinite strip, with only two scales in the x-direction.

According to the classical rule within the double scale expansion method, the following identities hold

$$\begin{aligned}
\partial_x &= q(\varepsilon)\partial_\xi + \varepsilon^{1/2}\partial_X = \partial_\xi + \varepsilon^{1/2}\partial_X + \varepsilon Q_1\partial_\xi + \varepsilon^{3/2}Q_2\partial_\xi + O(\varepsilon^2),\\
\partial_x^2 &= \partial_\xi^2 + 2\varepsilon^{1/2}\partial^2_{\xi X} + \varepsilon(\partial_X^2 + 2Q_1\partial_\xi^2) + 2\varepsilon^{3/2}(Q_1\partial^2_{X\xi} + Q_2\partial_\xi^2) + O(\varepsilon^2),\\
\Delta^2_{xy} &= \Delta^2_{\xi y} + 4\varepsilon^{1/2}\partial^2_{\xi X}\Delta_{\xi y} + 2\varepsilon\{(\partial_X^2 + 2Q_1\partial_\xi^2)\Delta_{\xi X} + 2\partial_\xi^2\partial_X^2\}\\
&\quad + 4\varepsilon^{3/2}\{(Q_1\partial^2_{X\xi} + Q_2\partial_\xi^2)\Delta_{\xi X} + \partial_X^3\partial_\xi + 2Q_1\partial_\xi^3\partial_X\} + O(\varepsilon^2),\\
[G,H]_{xy} &= [G,H]_{\xi y} + 2\varepsilon^{1/2}([\![\partial_X G, H]\!] + [\![\partial_X H, G]\!]) + O(\varepsilon),
\end{aligned}$$

where we have used the notations

$$\begin{aligned}
\Delta_{uv} &= \partial_u^2 + \partial_v^2,\\
[\![G,H]\!] &= (\partial_\xi G)(\partial_y^2 H) - (\partial_y G)(\partial^2_{\xi y} H),
\end{aligned} \tag{15}$$

and where $[,]_{x,y}$ is the bilinear differential operator defined in (3). In what follows, we always consider the differential operators $[,]$ and Δ with respect to the rapid variables ξ, y, and therefore we omit the indices.

The deflection w and the stress function f are expanded into powers of $\varepsilon^{1/2}$

$$w = \varepsilon^{1/2}w_1 + \varepsilon w_2 + \varepsilon^{3/2}w_3 + \varepsilon^2 w_4 + O(\varepsilon^{5/2}), \tag{16}$$

$$f = \varepsilon f_2 + \varepsilon^{3/2} f_3 + O(\varepsilon^2). \tag{17}$$

For finite aspect ratio problems[4], w and f have similar expansions, but the term εw_2 vanishes because of symmetry. We shall show that it is necessary to account for spatial interactions. Inserting (16), (17) and the previous operational rules into the field equation (1), we find at the four first orders (with the notation $\square = \Delta^2 + 4\partial_\xi^2$)

$$\square w_1 = 0, \tag{18}$$

$$\square w_2 = -4\partial_{\xi X}^2(\Delta+2)w_1, \tag{19}$$

$$\square w_3 = -4\partial_{\xi X}^2(\Delta+2)w_2 - 2(\partial_X^2 + 2Q_1\partial_\xi^2)(\Delta+2)w_1 - \partial_\xi^2(4\partial_X^2+1)w_1 + [f_2, w_1], \tag{20}$$

$$\begin{aligned}\square w_4 = {} & -4\partial_{\xi X}^2(\Delta+2)w_3 - 2(\partial_X^2 + 2Q_1\partial_\xi^2)(\Delta+2)w_2 - 4(Q_1\partial_{X\xi}^2 + Q_2\partial_\xi^2)(\Delta+2)w_1 \\ & - \partial_\xi^2(4\partial_X^2+1)w_2 - 4\partial_X^3\partial_\xi w_1 - 8Q_1\partial_\xi^3\partial_X w_1 - 2\partial_{\xi X}^2 w_1 \\ & + [f_3, w_1] + [f_2, w_2] + 2[\![\partial_X f_2, w_1]\!] + 2[\![\partial_X w_1, f_2]\!].\end{aligned} \tag{21}$$

In the like manner, from eqn (2) we obtain

$$\Delta^2 f_2 = -[w_1, w_1]/2, \tag{22}$$

$$\Delta^2 f_3 = -4\partial_{X\xi}^2 \Delta f_2 - [w_1, w_2] - 2[\![\partial_X w_1, w_1]\!]. \tag{23}$$

The first-order equation (18) is to be solved with the boundary condition (4) and with the assumption of 2π-periodicity with respect to ξ. As in Section 2, the solutions are in the form

$$w_1(X, \xi, y) = \gamma A_1(X)\, e^{i\xi} \cos y + \text{c.c.}, \tag{24}$$

where the complex amplitude $A_1(X)$ is an arbitrary function of the slow variable because only the rapid variables ξ and y appear in the differential operator $\square$. The real number γ has been introduced for the sake of normalization. With this w_1, eqn (19) is identical to (18), and its solution involves a second order slowly varying amplitude $A_2(X)$

$$w_2(X, \xi, y) = \gamma A_2(X)\, e^{i\xi} \cos y + \text{c.c.} \tag{25}$$

The stress functions f_2 and f_3 are uniquely defined by eqns (22) and (23), the boundary conditions (5) and the requirement of 2π-periodicity. They can be explicitly expressed as functions of the unknown amplitudes $A_1(X)$, $A_2(X)$. This computation is performed in Appendix A. For instance, the first term f_2 is given by

$$\begin{aligned} f_2(X, \xi, y) &= -\gamma^2 |A_1|^2 \cos^2 y/8 + \gamma^2 A_1^2\, e^{2i\xi} g(y)/16 + \text{c.c.}, \\ g(y) &= -1 + a \cosh(2y) + by \sinh(2y), \\ a &= \frac{\sinh\pi + \pi\cosh\pi}{\pi + \sinh\pi\cosh\pi}, \qquad b = -\frac{2\sinh\pi}{\pi + \sinh\pi\cosh\pi}. \end{aligned} \tag{26}$$

On account of (24)–(26), eqn (20) has the form

$$\square w_3 = F_1(y)\, e^{i\xi} + F_3(y)\, e^{3i\xi} + \text{c.c.} \tag{27}$$

The square operator $\Box$, associated with (4) and with the periodicity condition, is selfadjoint, and its kernel is given by (10). Hence, the nonhomogeneous equation (27) has a solution if and only if the right-hand side of (27) satisfies the solvability condition

$$\int_{-\pi/2}^{+\pi/2} F_1(y) \cos y \, dy = 0. \tag{28}$$

As shown in Appendix B, this solvability condition provides a differential equation for the first amplitude A_1

$$4A_1'' + A_1 - A_1|A_1|^2 = 0, \tag{29}$$

where the nonlinear term has been simplified by choosing the number γ in such a way that

$$\gamma^2 = \frac{2\pi(\pi + \sinh \pi \cosh \pi)}{\pi^2 + \pi \sinh \pi \cosh \pi - \sinh^2 \pi} \approx 2.897929. \tag{30}$$

The fundamental equation (29) first appeared in papers by Newell and Whitehead[16] and Segel[15] and has been found in a number of stability problems[17, 23].

In the same way, there is a solvability condition for the existence of w_4. This leads to a differential equation for $A_2(X)$ (Appendix B)

$$4A_2'' + A_2 - 2|A_1|^2 A_2 - A_1^2 \bar{A}_2 = 4iA_1''' - 8iQ_1 A_1' + 2iA_1' - i\gamma^2 \delta |A_1|^2 A_1', \quad \delta \approx 1.132523. \tag{31}$$

This second amplitude equation has been recently established for problems of convection[18] and beam buckling[20, 22].

Similar computations are performed with the less realistic boundary conditions (6) in Appendix C. The results do not corroborate exactly those of Pomeau[23].

4. CLAMPED SHORT SIDES

In this section we consider short sides that are perfectly or imperfectly clamped. The deflection satisfies (7) and (8) with a nonnegative coefficient k. The plate is clamped in the usual sense if k is zero. In the general case, the supports of the short sides have an elastic behaviour with respect to the plate rotation, and k is the compliance.

We assume that the expansions (13), (14), (16), (24) and (25) hold up to the boundary $x = 0$. Close to this boundary, which means in the region $x = O(1)$ or $X = O(\varepsilon^{1/2})$, these expansions can be written in the form

$$w(x, y) = \gamma \, e^{ix} \cos y \{\varepsilon^{1/2} A_1(0) + \varepsilon(A_1'(0)x + A_2(0))\} + \text{c.c.} + O(\varepsilon^{3/2}). \tag{32}$$

At the first order the deflection is harmonic. Because w and $\partial_x w - \partial_x^2 w k$ are not in phase, both conditions (7) and (8) cannot be satisfied except if the amplitude $A_1(0)$ is zero. The same holds at the other short sides

$$A_1(0) = A_1(L\varepsilon^{1/2}) = 0. \tag{33}$$

An alternative type of solution (referred to as a type II solution) has been studied by Kramer and Hohenberg[21], who assumed that the expansions no longer hold for small X's. This has been performed for a one-dimensional model with a negative compliance. If k is negative, it seems that local buckling appears at a load much smaller than λ_c. Hence, for λ close to λ_c, the deflection is large close to the short sides, and type II solutions are relevant. In the present case of a positive k, it does not seem restrictive to suppose that the deflection remains small in the region of $x = O(1)$.

Equations (29) and (33) govern the evolution of the first amplitude $A_1(X)$ when the

load increment ε increases. Their classical treatment[16, 18] is recalled for the sake of completeness. It is convenient to introduce the amplitude and the phase

$$A_1(X) = r(X)\, e^{i\theta(X)}.$$

Hence eqns (29) may be integrated

$$r^2\theta' = Q, \tag{34}$$

$$4r'^2 = r^2 - r^4/2 + 4Q^2/r^2 + E, \tag{35}$$

where Q and E are constants of integration. Because of the boundary conditions (33), the real amplitude $r(X)$ is zero at the boundaries $X = 0$, $L\varepsilon^{1/2}$. By virtue of (34) the constant Q is zero, and the phase $\theta(X)$ is constant. This means that the boundary conditions prevent a variation of the wavenumber at the order $\varepsilon^{1/2}$. We establish later on that the phase is more slowly modulated.

We now study the evolution of the shape of the real amplitude $r(X)$. A solution branch bifurcates from the trivial one $r = 0$ when there exist nonzero solutions of the linearized equation

$$4r'' + r = 0, \qquad r(0) = r(L\varepsilon^{1/2}) = 0. \tag{36}$$

The first bifurcation value $\varepsilon_1 = (2\pi/L)^2$ is small because the length is large. The nonlinear analysis of (35) is straightforward. The phase portrait is given in Fig. 3. Because of the boundary condition (33), only the closed curves are relevant. These solutions $r(X)$ are proportional to a Jacobian elliptic function, which is periodic[24]. It is pictured for various ε in Fig. 4, in the case where the amplitude has only a half-wave. Close to the bifurcation value ε_1, the amplitude is nearly $\{4(\varepsilon-\varepsilon_1)/3\varepsilon_1\}^{1/2} \sin(x/L)$, and the influence of the short sides spreads to the entire plate. For $\varepsilon/\varepsilon_1$ large—equivalently, εL^2 large—the amplitude in the centre of the plate is nearly equal to unity, that is, the maximal amplitude. Close to the short sides there are boundary layers of which the thickness is of order $\varepsilon^{-1/2}$ in terms of the initial variable x. Thus the size of these layers decays when the load increases. At this stage, the influence of a short side is limited to a decreasing region. The saddle–saddle

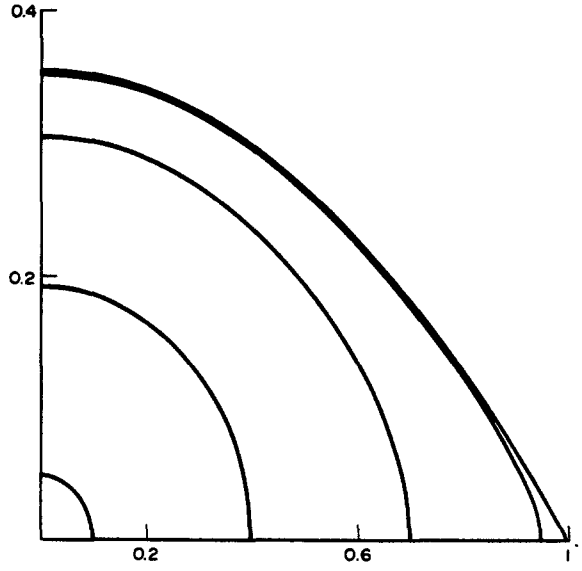

Fig. 3. Phase portrait in a quarter of plane. The pictured maximal amplitudes are 0.1, 0.4, 0.7, 0.95 and 0.995. The corresponding $\varepsilon/\varepsilon_1$ are 1.008, 1.13, 1.60, 3.95 and 9.06. The origin is a focus. The point (1, 0) is a saddle.

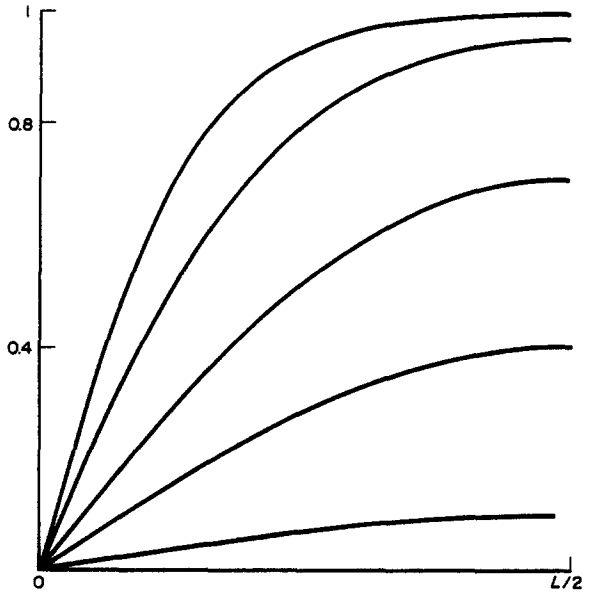

Fig. 4. Patterns amplitude along the half-plate for the same values of ε as in Fig. 3. A boundary layer appears for large ε.

loop of the phase portrait renders an account of this boundary layer. The corresponding complex amplitude

$$A_1(X) = e^{i\phi} \tanh(X/2^{3/2}) \tag{37}$$

satisfies $A_1(0) = 0$ and eqn (29) in the half-infinite domain $X > 0$. The possible values of the initial phase ϕ cannot be found at the present step of computation. The solution (37) of (29) first appeared in [24], and a very accurate coincidence has been observed by Wesfreid *et al.*[25] in an experiment of convection. There can be only a qualitative agreement with the plate experiment of Clement *et al.*[13] because the experimental aspect ratio (nine) was not sufficiently large. All solutions other than the previous one appear by bifurcation from the trivial solution at the values $\varepsilon_n = (2n\pi/L)^2$, n being an integer. They present n half-waves. When ε becomes large, the amplitude is nearly ± 1, except in the boundary layers and in $n-1$ internal walls where the solution is similar to (37). As it can be expected, these solutions with internal walls are unstable[24].

The previous analysis is sufficient for a load increment ε of order $1/L^2$, in which case it is not worth computing the Q_1 introduced in (14) because εx remains small everywhere in the plate. Henceforth we consider a larger ε, of order $1/L$ at least. We have just seen that, in this range, the postbuckling amplitude is nearly constant in the centre of the plate, and there are two boundary layers corresponding to solutions of (29) as in (37). Therefore it is consistent to begin with the half-infinite problem ($x > 0$).

By applying conditions (7) and (8) to the deflection w in the form (32) up to the order ε, we obtain

$$A_2(0) = A_1'(0)(i/2+k) + \overline{A_1'(0)}(i/2-k) = \alpha A_1'(0) + \beta \overline{A_1'(0)}. \tag{38}$$

The second order amplitude equation (31) can be rewritten as

$$\mathscr{L}(A_2) = h(x) = 4iA_1''' + 2iA_1' - 8iQ_1A_1' - i\gamma^2\delta|A_1|^2A_1', \tag{39}$$

where we have introduced the operator $\mathscr{L}(\cdot)$, which is linear with respect to real coefficients

$$\mathscr{L}(a) = 4a'' + a - 2|A_1(X)|^2 a - A_1^2(X)\bar{a}. \tag{40}$$

Since the first amplitude is given by (37), we easily find the asymptotic behaviour of the solutions $A_2(X)$ of (39) for large X's.

$$A_2(X) \sim e^{i\phi}(C_1\, e^{-X/\sqrt{2}} + C_2\, e^{X/\sqrt{2}} + iC_3 + iC_4 X).$$

Hence the requirement of a bounded $A_2(X)$ gives two equations ($C_2 = C_4 = 0$), that seem adequate in addition to the initial condition (38). But the linear operator $\mathscr{L}(\cdot)$ is singular, as can be seen by taking the derivative of eqn (29) with respect to the arbitrary phase ϕ

$$\mathscr{L}(iA_1) = 0. \tag{41}$$

This suggests that the solution of (38) and (39) is not bounded for any right-hand side of (39). The boundedness requirement will provide Q_1 as a function of ϕ. Let us introduce the bilinear form

$$\langle a, b\rangle = \int_0^\infty \{a(X)\bar{b}(X) + \text{c.c.}\}\, dX. \tag{42}$$

If $A_2(X)$ and the trial function $a(X)$ are bounded with vanishing derivatives for large X, the following identity is easily established by integration by parts

$$\langle \mathscr{L}(A_2), a\rangle - \langle \mathscr{L}(a), A_2\rangle = 8\ \text{Re}\ \{A_2(0)\overline{a'(0)} - A_2'(0)\overline{a(0)}\}. \tag{43}$$

We choose $a = iA_1$. On account of (38), (39), (41) and (43) and of the obvious identities

$$\langle iA_1', iA_1\rangle = 1, \qquad \langle iA_1''', iA_1\rangle = 1/8, \qquad \langle i|A_1|^2 A_1', iA_1\rangle = 1/2, \tag{44}$$

we find the first term Q_1 in the wavenumber expansion (14)

$$8Q_1 = 5/2 - \delta\gamma^2/2 - \text{Im}\ \alpha - \text{Im}(\beta\, e^{-2i\phi}). \tag{45}$$

With the numerical values of α, γ, δ in (30), (31) and (38), we obtain

$$Q_1 = 0.044877 - \text{Im}(\beta\, e^{-2i\phi})/8. \tag{46}$$

Hence the wavenumber variation $Q_1\varepsilon^{1/2}$ depends on the arbitrary phase ϕ that is introduced in (37). For the half-infinite problem, this phase remains indefinite, and there is a one-parameter family of solutions. Because of (46), Q_1 is restrained to lie in an interval. In terms of the original variable x, the interval of selected wavenumbers is

$$1 + Q_-\varepsilon + O(\varepsilon^{3/2}) \leqslant q \leqslant 1 + Q_+\varepsilon + O(\varepsilon^{3/2}), \qquad Q_\pm = 0.044877 \pm (1+4k^2)^{1/2}/16. \tag{47}$$

For the finite domain analysis, we refer to Cross *et al.*[18]. If εL is of order one, a similar family of solutions can be built up from the second short side $x = L$. Both families can be matched in the centre of the plate, which leads to an equation for the phase ϕ. Nevertheless, for εL sufficiently large, there is a large number of admissible wavenumbers that are distributed in the whole band (47). Daniels[26] has studied the stability of these solutions. He has established that the wavenumbers corresponding to stable solutions are also distributed in the same band.

There should be three qualitative behaviours, according to the signs of Q_- and Q_+. In the present case, Q_- is negative and Q_+ is positive, whatever the flexural compliance k of the supports at the short sides may be. Hence, the wavenumber may remain constant when the load increases, and the finite domain analysis[18] has shown that the variation of the wavenumber is not significant. But there are many other stable solutions, whose corresponding wavenumbers lie in the cone pictured in Fig. 5 and given by (47). To observe

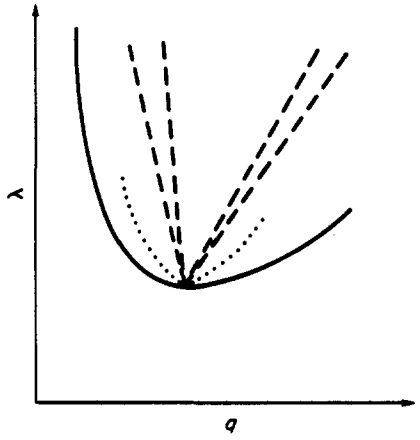

Fig. 5. Computed lower limits in the clamped case, for $k = 0.5$ (dashes) and in the supported case (dots). These results hold only for small load increment.

these solutions, it is necessary to carry out an alternative loading process. If one reduces the load from such a state whose wavenumber is different from the critical one, the wavenumber changes and goes to its critical value. According to the finite domain analysis, the basic mechanism of this wavenumber variation is a sequence of snap-through, whose number may be large. In other respects, formula (47) shows that the cone of admissible wavenumbers extends when the flexural compliance k increases, as is the case for beam buckling[20].

We remark that, with the alternative boundary conditions (6), Q_- is positive, as established in Appendix C. Then the wavelength necessarily decreases when the load increases. In this case, the sequence of snap-through exists also for an increasing load.

Our asymptotic method is similar to the one of Cross *et al.*[18], but they use the two scales X and x rather than X and ξ. With their method, one finds (39) with $Q_1 = 0$, and the boundedness condition is not satisfied. Using an identity like (43), one can compute the imaginary part of $A_2'(\infty)$, which is different from zero. Therefore the series (16) no longer holds for large X, so that a second asymptotic expansion and a matching are needed to obtain the selected wavenumbers. Our method permits us to avoid this step.

5. SIMPLY SUPPORTED SHORT SIDES

In this section, we consider briefly the case of simply supported short sides. The boundary conditions for the deflection at $x = 0, L$ are (7) and

$$\partial_x^2 w(0, y) = \partial_x^2 w(L, y) = 0. \tag{48}$$

The amplitude equations (29), (31) are still valid, but the second one will not be useful. The main change with respect to the clamped case relies on the fact that w and $\partial_x^2 w$ are in phase and, consequently, that the amplitude $A_1(X)$ does not vanish at the boundaries. If one requires the $(2\pi/q)$-periodicity in the $0x$-direction, the classical theory[3, 4] allows one to establish the existence of buckled solutions for a load greater than $\lambda(q)$. Because the boundary conditions are invariant under the change $x \to -x$, they may be satisfied by these periodic solutions, as was proved by an argument in [20], Part 1. Hence, there exist solutions for (q, λ) in the region above the neutral stability curve, and we now study their stability.

With account of (34), we can rewrite (35) as

$$4(r'' - r\theta'^2) + r - r^3 = 0. \tag{49}$$

We assume that the expansions (16) are valid up to the short sides. Therefore the boundary

conditions (7), (48) can be applied to (32), which leads to

$$\theta(0) = \pi/2, \qquad \theta(l) = (n+1/2)\pi - L, \tag{50}$$

$$r'(0) = r'(l) = 0, \tag{51}$$

where n is an integer and $l = L\varepsilon^{1/2}$. The periodic solutions of Von Karman equations correspond to the following family of solutions of (34), (49), (50) and (51)

$$r(X) = r_0, \qquad \theta(X) = QX + \pi/2, \tag{52}$$

$$Q = n\pi/l - \varepsilon^{-1/2} = (1 - r_0^2)^{1/2}/2. \tag{53}$$

If l is much larger than one, there are many admissible "wavenumbers" Q, which are densely distributed in the interval

$$Q^2 \leqslant 1/4. \tag{54}$$

This interval corresponds to the whole region above the neutral stability curve (11). The amplitude r_0 vanishes at the extremal values $Q = \pm 1/2$, which bears out that the neutral stability curve is a bifurcation locus for periodic solutions.

Von Karman equations derive from a potential energy. For the sake of simplicity, we reintroduce a sort of potential energy as follows: we multiply the amplitude equation (29) by functions $\overline{\delta A}(X)$ such that

$$\text{Re } \delta A_1(0) = \text{Re } \delta A_1(l) = 0$$

to be in accord with (50). Next we add the complex conjugate. On account of (51), we conclude that $A_1(X)$ is a stationary point of the functional

$$\Phi(A_1) = \int_0^l \left\{ 4|A_1'|^2 - |A|^2 + \frac{|A|^4}{2} \right\} \mathrm{d}X,$$

$$\Phi(r, \theta) = \int_0^l \left\{ 4r'^2 + 4r^2\theta'^2 - r^2 + \frac{r^4}{2} \right\} \mathrm{d}X. \tag{55}$$

If one drops the modulation of the amplitude and of the phase, the functional Φ should be compared with the potential energy obtained by the classical theory[3]. Then Φ appears as the potential energy divided by ε^2 and by a positive constant. Hence, the equilibrium states (52), (53) are stable if and only if they are local minima of Φ. Let us compute the second variation of Φ close to the states (52)

$$\delta^2\Phi = \int_0^l \{4\delta r'^2 + \delta r^2(4Q^2 + 3r_0^2 - 1) + 16r_0Q\delta r\delta\theta' + 4r_0^2\delta\theta'^2\} \, \mathrm{d}X. \tag{56}$$

In theory, the boundary conditions (50) restrict the admissible values of $\delta\theta'(X)$. Because the wavenumber Q in (53) varies almost continuously, it seems rational to consider $\delta\theta'(X)$ as unrestrained. Minimizing (56) with respect to the phase, we find

$$\delta\theta' = -2Q\delta r/r_0. \tag{57}$$

Inserting (57) into (56), we can put the stability test in the form

$$\delta^2\Phi = \int_0^l \{4\delta r'^2 + \delta r^2(3r_0^2 - 1 - 12Q^2)\} \, \mathrm{d}X \geqslant 0. \tag{58}$$

Because of (51), $\delta r(X)$ is unrestrained and condition (58) is equivalent to

$$3r_0^2 - 1 - 12Q^2 \geqslant 0. \tag{59}$$

On account of (53), we finally obtain

$$Q^2 \leqslant 1/12. \tag{60}$$

Hence, in the (λ, q) plane, the stable solutions occupy the region above a curve of parabolic shape

$$\lambda - \lambda_c = \lambda - 4 = 12(q-1)^2 + O(q-1)^3, \tag{61}$$

which is three times narrower than the neutral stability curve [compare (60) with (54)]. This type of wavelength selection by phase instability is known under the name of Eckhaus instability[27].

6. COMPARISON WITH OTHER THEORIES, COMPARISON WITH EXPERIMENTS

The classical postbuckling theory[3, 4] can be applied when the linear analysis provides a small number of instability modes, mainly when the aspect ratio is finite. This analysis also holds for an infinite plate if the wavenumber is *a priori* kept at its critical value. So the buckled deflections are in the form

$$w(x, y) = a \cos y \sin(x + \phi) + O(a^3), \tag{62}$$

where the amplitude a is related to the load increment ε by an algebraic equation [γ being given in (30)]

$$\varepsilon a - \gamma^2 a^3 = 0. \tag{63}$$

This usual method has been recently extended when there exist two nearly coincident instability modes, for instance with a simply supported plate whose aspect ratio r is close to $2^{1/2}$. The possible deflections combine the two modes $W_1(x, y)$ and $W_2(x, y)$

$$w(x, y) = a_1 W_1 + a_2 W_2 + O(|a|^3), \tag{64}$$

where the amplitudes a_1 and a_2 are solutions of the following two equations that involve numerical coefficients $\alpha_1 \cdots \gamma_2$

$$\begin{aligned} \{\alpha_1 a_1^2 + \beta a_2^2 - \varepsilon + \gamma_1 (r - 2^{1/2})\} a_1 &= 0, \\ \{\beta a_1^2 + \alpha_2 a_2^2 - \varepsilon + \gamma_2 (r - 2^{1/2})\} a_2 &= 0. \end{aligned} \tag{65}$$

According to the values of the coefficients, these equations account for several postbuckling behaviours that often include secondary bifurcations. With the present boundary conditions (5), the two modes ($a_1 = 0$ or $a_2 = 0$) are stable for ε much larger than $|r - 2^{1/2}|$[9]. Then the two wavelengths can be observed. With the alternative boundary conditions (6), only the shorter wavelength is selected[10].

As for the problem studied in the present paper, there exists an infinite packet of instability modes. To take the whole packet into account, we used the double scale expansion method, as it is classically used within the field of hydrodynamic instabilities. In particular, we followed the ideas of the excellent paper of Cross *et al.*[18]. In comparison with (62), the deflection of the clamped plate is modulated by a slowly varying amplitude, whose shape depends on the load increment (Fig. 4). For finite εL the deflection in the left half-plate is written as (see also Fig. 6)

$$w(x, y) = \gamma \varepsilon^{1/2} \tanh(x(\varepsilon/8)^{1/2}) \cos(qx + \phi) \cos y + O(\varepsilon). \tag{66}$$

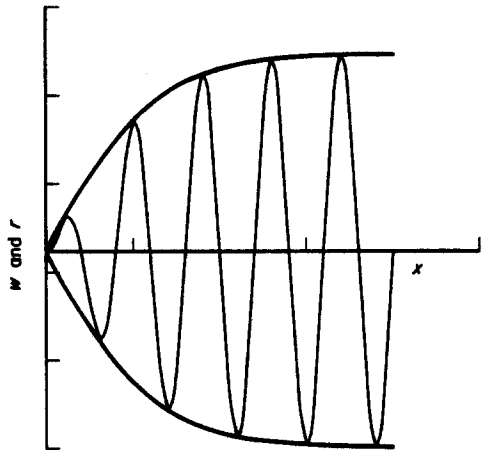

Fig. 6. Amplitude r and deflection w in the boundary layer.

Hence, the amplitude of the oscillations varies in a boundary layer whose width is of order $\varepsilon^{-1/2}$ and, therefore, decreases when the load increases. For large εL, there are many solutions that are characterized by their initial phase ϕ. The wavenumber q depends on ϕ, and it is restricted to lie in a band of width ε, which is given by (47). It is important to remark that the band of admissible wavenumbers increases with the flexibility of supports k (Fig. 5). The computation of this band is the main result of this paper, because the postbuckling behaviour follows from it in the range $\varepsilon = O(1/L)$. The wavenumber may remain constant with an increasing loading, but one may observe a sequence of snaps with a decreasing loading, as explained in Section 4. With the alternative boundary conditions (6), the band of admissible wavenumbers is computed in Appendix C. It has been established that the wavelength must decrease when the load increases. It is noteworthy that these two results are qualitatively equivalent to those previously quoted in the case of an aspect ratio close to $2^{1/2}$, but any general inference should be reckless. A short account of our computations has been published in [22], but the reader should be aware that the numerical values of $Q_{\pm}$ were wrong.

For a simply supported plate it is not worth introducing an amplitude modulation. A stability analysis with respect to changes of the wavenumber permits one to select a band of admissible wavenumbers which is larger than in the clamped case (Fig. 5)

$$|q-1| \leqslant \{\varepsilon/12\}^{1/2} + O(\varepsilon). \tag{67}$$

Most of our results are in qualitative agreement with the experiments[13, 14]. But the experimental band of admissible wavenumbers does not coincide with (47), even if there is a better fit than with a previous study[23]. A too-definite comparison would not be significant because the experimental aspect ratios (eight, nine) are not sufficiently large. In this respect, new experiments are needed. A second reason makes doubtful the comparison in the clamped case. Indeed our starting equation (1) assumes a uniform and uniaxial prebuckling stress, which is wrong near the clamped sides. Nevertheless, eqn (1) and the analysis of Section 3 remain valid outside the regions $x = O(1)$, $L-x = O(1)$. Hence, it is likely that only the numerical values of the coefficients α, β in (38) would be altered after having accounted for the nonuniformity of the prebuckling stress.

REFERENCES

1. S. P. Timoshenko and J. M. Gere, *Theory of Elastic Stability*. McGraw-Hill, New York (1961).
2. D. O. Brush and B. O. Almroth, *Buckling of Bars, Plates and Shells*. McGraw-Hill, New York (1975).
3. W. T. Koiter, On the stability of elastic equilibrium. Thesis, Delft (1945). English translation: NASA Techn. Transl. F 10, 833 (1967).

4. B. Budianski, Theory of buckling and postbuckling behaviour of elastic structures. *Adv. Appl. Mech.* **14**, 1–65 (1974).
5. A. Langenbach and L. Recke, On perturbation of branching problems and secondary branching in the theory of plates. *Abh. Akad. Wiss. D.D.R. Math.* Nr. 2N, 165–179 (1981).
6. S. E. List, Generic bifurcation with applications to the Von Karman equations. *J. Diff. Equations* **30**, 89–118 (1978).
7. B. J. Matowsky, L. J. Putnick and E. L. Reiss, Secondary states of rectangular plates. *SIAM J. Appl. Math.* **38**, 38–51 (1980).
8. T. Nakamura and K. Uetani, The secondary and postsecondary buckling behaviours of rectangular plates. *Int. J. Mech. Sci.* **21**, 265–286 (1979).
9. M. Potier-Ferry, Multiple bifurcation, symmetry and secondary bifurcation. In *Nonlinear Problems of Analysis in Geometry and Mechanics* (Edited by D. Atteia, D. Bancel and I. Gumovski), pp. 158–167. Pitman, Boston (1981).
10. D. Schaeffer and M. Golubitsky, Boundary conditions and mode jumping in the buckling of a rectangular plate. *Comm. Math. Phys.* **69**, 209–236 (1979).
11. L. Bauer and E. L. Reiss, Nonlinear buckling of rectangular plates. *J. Soc. Ind. Appl. Math.* **13**, 603–627 (1965).
12. M. Uemura and O. J. Byon, Secondary buckling of a flat plate under uniaxial compression. Part 2: analysis of clamped plate by F.E.M. and comparison with experiments. *Int. J. Nonlinear Mech.* **12**, 355–370 (1977).
13. M. Clement, E. Guyon and J. E. Wesfreid, Multiplicité des modes de déformation d'une plaque sous compression. *C.R. Acad. Sci. Paris* Sér. II **293**, 87–89 (1981).
14. M. Boucif, E. Guyon and J. E. Wesfreid, Role of boundary conditions on mode selection in a buckling instability. *J. Phys. Lett.* **45**, L-413–L-418 (1984).
15. L. Segel, Distant sidewalls cause slow amplitude modulation of cellular convection. *J. Fluid Mech.* **38**, 203–224 (1969).
16. A. C. Newell and J. A. Whitehead, Finite bandwidth, finite amplitude convection. *J. Fluid Mech.* **38**, 279–303 (1969).
17. C. G. Lange and A. C. Newell, The postbuckling problem for thin elastic shells. *SIAM J. Appl. Math.* **21**, 605–629 (1971).
18. M. C. Cross, P. G. Daniels, P. C. Hohenberg and E. D. Siggia, Phase-winding solutions in finite container above the convective threshold. *J. Fluid Mech.* **127**, 155–183 (1983).
19. Y. Pomeau and S. Zaleski, Wavelength selection in one-dimensional cellular structures. *J. Phys.* **42**, 515–528 (1981).
20. M. Potier-Ferry, Amplitude modulation, phase modulation and localization of buckling patterns. In *Collapse* (Edited by J. M. T. Thompson and G. W. Hunt), pp. 149–159. Cambridge Univ. Press, Cambridge (1983).
21. L. Kramer and P. C. Hohenberg, Effect of boundary conditions on wavenumber selection in spatially varying steady states. In *Cellular Structures in Instability Problems* (Edited by J. E. Wesfreid and S. Zaleski), pp. 63–74. Lecture Notes in Physics, Springer-Verlag, Berlin (1984)
22. M. Potier-Ferry, Wavelength selection and pattern localization in buckling problems. In *Cellular Structures in Instability Problems* (Edited by J. E. Wesfreid and S. Zaleski), pp. 43–55. Lecture Notes in Physics, Springer-Verlag, Berlin (1984).
23. Y. Pomeau, Nonlinear pattern selection in a problem of elasticity. *J. Phys. Lett.* **42**, L1 (1981).
24. P. G. Daniels, The effect of distant sidewalls on the transition to finite amplitude Bénard convection. I, II. *Proc. R. Soc. London A* **358**, 173–197 (1977); *Mathematika* **25**, 216–235 (1978).
25. J. E. Wesfreid, Y. Pomeau, M. Dubois, C. Normand and P. Berge, Critical effects in Rayleigh-Bénard convection. *J. Phys.* **39**, 725–731 (1978).
26. P. G. Daniels, The effect of distant sidewalls on the evolution and stability of finite amplitude Rayleigh-Bénard convection. *Proc. R. Soc. London A* **378**, 539–566 (1981).
27. W. Eckhaus, *Studies in Nonlinear Stability Theory*. Springer Tracts in Natural Philosophy, No. 6. New York (1965).

APPENDIX A

We compute the first two terms, f_2 and f_3, of the stress function, which depend on the amplitudes $A_1(X)$, $A_2(X)$ and on the normalization factor γ. We recall that the $f_i(X, \xi, y)$'s must be 2π-periodic with respect to ξ, and they must satisfy the boundary conditions (5). These requirements are implicit in what follows. Let us introduce the function

$$U(\xi, y) = e^{i\xi} \cos y, \tag{A1}$$

which generates (with $\bar{U}$) the kernel of the operator $\square$. Let us note the identities

$$[U, \bar{U}] = 2 \cos 2y, \tag{A2}$$

$$[U, U] = 2e^{2i\xi}. \tag{A3}$$

Then, with the w_1, w_2 given in (24), (25), eqn (22) can be written as

$$\Delta^2 f_2 = -\gamma^2(A_1^2 e^{2i\xi} + |A_1|^2 \cos 2y + \text{c.c.}). \tag{A4}$$

For convenience, let $g_0(y)$ and $g(y)$ be the solutions of

$$\Delta^2 g_0 = 16 \cos 2y \Rightarrow g_0(y) = 1 + \cos 2y, \tag{A5}$$

$$\Delta^2(g\,e^{2i\xi}) = 16e^{2i\xi} \Rightarrow g(y) \qquad \text{given by (26).} \tag{A6}$$

Hence, the solution of (A4) is

$$f_2(X,\xi,y) = -\{|A_1|^2(1+\cos 2y)+A_1^2 e^{2i\xi} g(y)+\text{c.c.}\}\gamma^2/16. \tag{A7}$$

Next we compute the r.h.s. of (23), with account of (5), (24), (25), (26), (A2), (A3), (A7) and of the following two results

$$[U,U] = -ie^{2i\xi}, \tag{A8}$$

$$[U,\bar{U}] = -[\bar{U},U] = -i\cos 2y, \tag{A9}$$

the nonsymmetric operator $[\,,\,]$ being defined in (15). We obtain thus

$$[w_1,w_2] = 2\gamma^2(A_1A_2e^{2i\xi}+A_1\bar{A}_2\cos 2y+\text{c.c.}), \tag{A10}$$

$$4\partial_\xi\partial_X\Delta f_2 = 4i\gamma^2A_1A_1'e^{2i\xi}(1+b\cosh 2y)+\text{c.c.}, \tag{A11}$$

$$2[\partial_X w_1,w_1] = -2i\gamma^2(A_1A_1'e^{2i\xi}+A_1'\bar{A}_1\cos 2y+\text{c.c.}). \tag{A12}$$

Equation (23) can be written as

$$\Delta^2 f_3 = -2\gamma^2\{(A_1A_2+iA_1A_1'(1+2b\cosh 2y))e^{2i\xi}+(A_1\bar{A}_2-iA_1'\bar{A}_1)\cos 2y+\text{c.c.}\}. \tag{A13}$$

To solve (A13), we need the solution $h(y)$ of

$$\Delta^2(h(y)\,e^{2i\xi}) = 16\cosh(2y)\,e^{2i\xi}, \tag{A14}$$

which is

$$h(y) = y^2\cosh(2y)/2+c\cosh 2y+dy\sinh 2y,$$
$$c = \frac{\pi^2(\sinh\pi\cosh\pi-\pi)}{8(\sinh\pi\cosh\pi+\pi)}, \qquad d = -\frac{\pi\cosh^2\pi}{2(\sinh\pi\cosh\pi+\pi)}. \tag{A15}$$

Then the solution of (A13) is

$$f_3 = -\tfrac{1}{8}\{(A_1A_2+iA_1A_1')g(y)e^{2i\xi}+2biA_1A_1'h(y)e^{2i\xi}+\text{c.c.}$$
$$+(1+\cos 2y)(A_1\bar{A}_2+\bar{A}_1A_2-iA_1'\bar{A}_1+i\bar{A}_1'A_1)\}\gamma^2. \tag{A16}$$

Similarly as in (5), the stress function must satisfy

$$f(0,y) = \partial_x f(0,y) = 0, \tag{A17}$$

which is not consistent with the solution (17), (A7), (A16). This means that the expansion (17) does not hold up to the short sides. The stress function has to be corrected in a sidewall region of width $x = O(1)$, but this correction does not alter either the amplitude equations that are valid in the region $X = O(1)$ (hence x large) or the sidewall deflection (32) that permits us to find the amplitude boundary conditions (33), (38).

APPENDIX B

Here we establish the two amplitude equations (29), (31), which follow from the solvability conditions for the existence of w_3 and w_4. After having introduced the mean value $\langle\langle\cdot\rangle\rangle$ on the rectangle $(0,2\pi)\times(-\pi/2,+\pi/2)$, we can write the solvability condition for an equation $\Box w = F(\xi,y)$

$$\langle\langle F\bar{U}\rangle\rangle = \frac{1}{2\pi^2}\int_0^{2\pi}\left\{\int_{-\pi/2}^{+\pi/2}F(\xi,y)\bar{U}(\xi,y)\,dy\right\}d\xi = 0. \tag{B1}$$

Of course, (B1) is equivalent to (28), which implies that the solvability condition proceeds only from the term $e^{i\xi}(\cdots)$ in the Fourier expansion of $F(\cdot,y)$.

Because $(\Delta+2)w_1$ and $(\Delta+2)w_2$ are zero, eqn (20) is reduced to

$$\Box w_3 = [f_2,w_1]+\gamma\{(4A_1''+A_1)U+\text{c.c.}\}. \tag{B2}$$

After several integrations by parts, one establishes that, for any 2π-periodic functions $v(\cdot,y)$, $w(\cdot,y)$ that are zero for $y = \pm\pi/2$, one has

$$\langle\langle[f,w]v\rangle\rangle = \langle\langle[w,v]f\rangle\rangle. \tag{B3}$$

With account of (A2), (A3), (A7), (B1), (B2), (B3), and of the obvious identity

$$\langle\langle |U|^2 \rangle\rangle = 1/2, \tag{B4}$$

the solvability condition for (20) can be put in the form

$$4A_1'' + A_1 - A_1|A_1|^2\gamma^2(1+\langle\langle g\rangle\rangle)/4 = 0, \tag{B5}$$

which is equivalent to (20) if one sets

$$\gamma^2 = 4/(1+\langle\langle g\rangle\rangle). \tag{B6}$$

The calculation of the mean value of g leads to the γ^2 given in (30). It will not be necessary to solve completely (B2).

With the w_1, w_2 in (24), (25) and with the definition of I

$$I(X,\xi,y) = (4A_2'' + A_2 - 4iA_1''' + 8iQ_1A_1' - 2iA_1')\gamma U(\xi,y) + \text{c.c.}, \tag{B7}$$

eqn (21) becomes

$$\square w_4 = I - 4\partial_{\xi X}^2(\Delta+2)w_3 + [\![f_2, w_2]\!] + [\![f_3, w_1]\!] + 2[\![\partial_X f_2, w_1]\!] + 2[\![\partial_X w_1, f_2]\!]. \tag{B8}$$

Using the same conditions as for (B3), we establish by integrations by parts the following identities

$$\langle\langle [\![f, w]\!] U\rangle\rangle = -\langle\langle [\![U, w]\!] f\rangle\rangle, \tag{B9}$$

$$\langle\langle [\![w, f]\!] U\rangle\rangle = \langle\langle f\{[\![w, U]\!] - [\![U, w]\!]\}\rangle\rangle, \tag{B10}$$

$$\langle\langle \bar{U}\partial_{\xi X}^2(\Delta+2)w_3\rangle\rangle = \langle\langle \partial_{\xi X}^2 w_3(\Delta+2)\bar{U}\rangle\rangle = 0. \tag{B11}$$

As consequences of (A2), (A3), (A7), (A8), (A9), (A16), (B3), (B9), (B10), we find

$$\langle\langle [f_2, w_2]\bar{U}\rangle\rangle = -\{|A_1|^2A_2 + A_1^2\bar{A}_2\langle\langle g\rangle\rangle\}\gamma^3/8, \tag{B12}$$

$$\langle\langle [f_3, w_1]\bar{U}\rangle\rangle = -\tfrac{1}{8}\{2(|A_1|^2A_2 + i|A_1|^2A_1')\langle\langle g\rangle\rangle + 4ib|A_1|^2A_1'\langle\langle h\rangle\rangle + A_1^2\bar{A}_2 + |A_1|^2A_2 - i|A_1|^2A_1' + iA_1^2\bar{A}_1'\}\gamma^3, \tag{B13}$$

$$2\langle\langle [\![\partial_X f_2, w_1]\!]\bar{U}\rangle\rangle = \tfrac{1}{8}\{A_1^2\bar{A}_1' + |A_1|^2A_1' + 2|A_1|^2A_1'\langle\langle g\rangle\rangle\}i\gamma^3, \tag{B14}$$

$$2\langle\langle [\![\partial_X w_1, f_2]\!]\bar{U}\rangle\rangle = |A_1|^2A_1'i\gamma^3/4. \tag{B15}$$

Gathering (B1), (B4), (B7), and (B11) to (B14), we obtain the solvability condition for (B8) as

$$4A_2'' + A_2 - 2|A_1|^2A_2 - A_1^2\bar{A}_2 = 4iA_1''' - 8iQ_1A_1' + 2iA_1' + i|A_1|^2A_1'\gamma^2(b\langle\langle h\rangle\rangle - 1). \tag{B16}$$

One computes easily the mean value of the function $h(y)$ defined in (A14) or (A15)

$$\langle\langle h\rangle\rangle = \sinh\pi(1/4-d)/\pi - (\cosh\pi)/2 \approx 0.78612. \tag{B17}$$

On account of (B17), (26), (30), the amplitude equation (B16) is identical to that written in (31).

APPENDIX C

After few changes, the calculations of Appendixes A and B hold for the boundary conditions (6). We relate that in detail to compare with the result of Pomeau[23]. The field equations (18) to (23) need not be altered. The stress functions (A7) and (A16) and the amplitude equations (29), (31) keep the same form if one replaces (26), (30), (31) by

$$g(y) = 1 \quad \text{or} \quad a = b = 0, \tag{C1}$$

$$\gamma^2 = 2, \tag{C2}$$

$$\delta = 1. \tag{C3}$$

The latter two are obvious consequences of (C1), (B6), (B16). Note that it is not necessary to compute $h(y)$, and that the boundary conditions (6) lead to drop the hyperbolic functions in the solution of (22), (23).

The numerical values of $Q_\pm$ (see (47)) are easily found

$$Q_\pm = 1/8 \pm (1+4k^2)^{1/2}/16. \tag{C4}$$

In the case of perfectly clamped short sides, one has

$$Q_- = 1/16, \qquad Q_+ = 3/16, \tag{C5}$$

and these values are twice those found in [23].